

Fast Alternating Projections on Manifolds Based on Tangent Spaces

Guang-Jing Song* Michael K. Ng†

March 24, 2020

Abstract

In this paper, we study alternating projections on nontangential manifolds based on the tangent spaces. The main motivation is that the projection of a point onto a manifold can be computational expensive. We propose to use the tangent space of the point in the manifold to approximate the projection onto the manifold in order to reduce the computational cost. We show that the sequence generated by alternating projections on two nontangential manifolds based on tangent spaces, converges linearly to a point in the intersection of the two manifolds where the convergent point is close to the optimal solution. Numerical examples for nonnegative low rank matrix approximation and low rank image quaternion matrix (color image) approximation, are given to demonstrate that the performance of the proposed method is better than that of the classical alternating projection method in terms of computational time.

Keywords: Alternating projection method, manifolds, tangent spaces, nonnegative matrices, low rank, nonnegativity, quaternion matrices

AMS subject classifications. 15A23, 65f22.

1 Introduction

Throughout this paper, let \mathcal{K} be a finite dimensional Hilbert space over \mathbb{R} , \mathcal{M}_1 and \mathcal{M}_2 be two manifolds included in \mathcal{K} . The corresponding projection operators on \mathcal{M}_1 , \mathcal{M}_2 and $\mathcal{M} = \mathcal{M}_1 \cap \mathcal{M}_2$ are denoted by π_1, π_2 and π respectively. In this paper, we are interested to determine a solution defined by π onto \mathcal{M} . For example, nonnegative rank r matrix approximation for nonnegative matrices aims to find a nonnegative rank r matrix such that the distance between such matrix and the

*School of Mathematics and Information Sciences, Weifang University, Weifang 261061, P.R. China. (email: sgjshu@163.com)

†Department of Mathematics, The University of Hong Kong, Pokfulam, Hong Kong (email: mng@maths.hku.hk). M. Ng's research supported in part by the HKRGC GRF 12306616, 12200317, 12300218 and 12300519, and HKU 104005583.

given nonnegative matrix is as small as possible. Here \mathcal{M}_1 refers to the set of rank r real matrices, \mathcal{M}_2 refers to the set of matrices with nonnegative entries, and the projection refers to the closest matrix to the given nonnegative matrix A , i.e.,

$$\pi(A) = \operatorname{argmax}_{X \in \mathcal{M}} \|A - X\|_F^2, \quad \pi_1(A) = \operatorname{argmax}_{X \in \mathcal{M}_1} \|A - X\|_F^2, \quad \pi_2(A) = \operatorname{argmax}_{X \in \mathcal{M}_2} \|A - X\|_F^2. \quad (1)$$

The classical alternating projection method is to determine a solution by using two projections π_1 onto \mathcal{M}_1 and π_2 onto \mathcal{M}_2 iteratively. The method is widely used in many fields, for instance in signal processing [7], finance [16], machine learning [30], numerical linear algebra [6], image processing [12, 13, 23], and other applications (see [11, 14, 17, 19, 20] and references therein). In the literature, Schwarz [26] firstly studied the alternating projection method. When \mathcal{M}_1 and \mathcal{M}_2 are affine linear manifolds, von Neumann [22] proved that the sequence derived by the alternating projection method is globally convergent to a solution given by the projection onto $\mathcal{M} = \mathcal{M}_1 \cap \mathcal{M}_2$ under the assumption that $\mathcal{M} \neq \emptyset$. And the convergence rate is shown to be linear and governed by the angle between \mathcal{M}_1 and \mathcal{M}_2 . However, when \mathcal{M}_1 and \mathcal{M}_2 are nonlinear manifolds, the corresponding results cannot be derived in general, i.e., even if $\mathcal{M}_1 \cap \mathcal{M}_2 \neq \emptyset$, the sequence generated by the alternating projection method is not necessary to be convergent. Lewis and Malick [21] studied the alternating projection method on two smooth manifolds which can be approximated by some affine subspaces. They proved that if the two manifolds intersect transversally, the sequence can be expected to be convergent to a point in the intersection of the two manifolds with a linear rate. Recently, Andersson and Carlsson [2] showed that if the two manifolds have “nontangential” intersection points, the sequence of alternating projections converges linearly to a point in the intersection which is sufficiently close to the optimal solution.

In the alternating projection method, the optimal solution of each projection is assumed. In general, the computational cost of each projection can be expensive. The main aim of this paper is to propose to use the tangent space of the point in the manifold to approximate the projection onto the manifold in order to reduce the computational cost. We show that the sequence generated by alternating projections on two nontangential manifolds based on tangent spaces, converges linearly to a point in the intersection of the two manifolds where the convergent point is close to the optimal solution. As an application, we demonstrate the proposed algorithm to solve nonnegative low rank matrix approximation to nonnegative matrices. We also present numerical examples for nonnegative low rank matrix approximation and low rank color image approximation, and demonstrate that the performance of the proposed method is better than that of other testing methods in terms of computational time.

The rest of this paper is organized as follows. In Section 2, we present the proposed tangent space-based alternating projection method. Nonnegative low rank matrix approximation problem is used as an example for illustration. In Section 3, we show the convergence of the proposed tangent space-based alternating projection

method. In Section 4, numerical examples are given to show the advantages of the proposed method. Finally, some concluding remarks are given in Section 5.

2 The Proposed Projection Method

2.1 Preliminaries

In this subsection, we first provide a review of some necessary concepts and preliminaries of the differential geometry (for details, we refer to [3]). Let \mathcal{K} be a Euclidean space, i.e., a Hilbert space of finite dimension $n \in \mathbb{N}$. Given $A \in \mathcal{K}$ and $r > 0$, we write $\mathcal{B}(A, r)$ for the open ball centered at A with radius r . Any subset \mathcal{M} of \mathcal{K} will be given the induced topology from \mathcal{K} . Let $p \geq 1$, and let $\mathcal{M} \subseteq \mathcal{K}$ be an m -dimensional \mathbb{C}^p -manifold. We recall that around each $A \in \mathcal{M}$, there exist an injective \mathbb{C}^p -immersion ϕ on an open set U in \mathbb{R}^m such that

$$\mathcal{M} \cap \mathcal{B}(A, s) = \text{Im } \phi \cap \mathcal{B}(A, s) \quad (2)$$

for some $s > 0$, where $\text{Im}(\phi)$ denotes the image of ϕ . If $A = \phi(x_A)$, we define the tangent space $T_{\mathcal{M}}(A)$ by

$$T_{\mathcal{M}}(A) = \text{Range } d\phi(x_A),$$

where *Range* refers to the range space and $d\phi$ denotes the Jacobian matrix. This property is very important which is saying that the tangent space $T_{\mathcal{M}}(A)$ provides a local vector space approximation of the manifold \mathcal{M} . It is well known that this definition of tangent space is independent of ϕ . Moreover, we set

$$\tilde{T}_{\mathcal{M}}(A) = T_{\mathcal{M}}(A) + A,$$

i.e., $\tilde{T}_{\mathcal{M}}(A)$ is the affine linear manifold which is tangent to \mathcal{M} at A . Let the map ϕ be given as in (2). Suppose that $A = \phi(x_A) \in \text{Im}(\phi)$, the projection onto the tangent space of \mathcal{M} at A can be written as $P_{T_{\mathcal{M}}(A)} = M(M^*M)^{-1}M^*$, where $M = d\phi(\phi^{-1}(A))$. Then the following result can be derived by the continuous of $d\phi$ and ϕ^{-1} .

Proposition 2.1 (Proposition 2.2 in [2]). *Let \mathcal{M} be a \mathbb{C}^1 -manifold. Then $P_{T_{\mathcal{M}}(A)}$ is a continuous function of A .*

The following proposition shows that the projections listed in (1) are locally well-defined.

Proposition 2.2 (Proposition 2.3 in [2]). *Let \mathcal{M} be a \mathbb{C}^2 -manifold, and let $A \in \mathcal{M}$ be given. Then there exists an $s > 0$ such that for all $B \in \mathcal{B}_{\mathcal{K}}(A, s)$, there exist a unique closest point in \mathcal{M} . Denoting this point by $\pi(B)$, the map $\pi : \mathcal{B}_{\mathcal{K}}(A, s) \rightarrow \mathcal{M}$ is \mathbb{C}^2 . Moreover, $C \in \mathcal{M} \cap \mathcal{B}_{\mathcal{K}}(A, s)$ equals $\pi(B)$ if and only if $B - C \perp T_{\mathcal{M}}(C)$.*

2.2 The Alternating Projection Method

It is well known that the convergence speed of the alternating projection method on linear manifolds is linear and decided by the angle between the two linear manifolds. Then, in order to generalize the alternating projection method to nonlinear manifolds, we first need to introduce the angle between two nonlinear manifolds. In this paper, the angle $\alpha(A)$ of $A \in \mathcal{M} = \mathcal{M}_1 \cap \mathcal{M}_2$ is defined as

$$\alpha(A) = \cos^{-1}(\sigma(A)) \text{ and } \sigma(A) = \lim_{\xi \rightarrow 0} \sup_{B_1 \in F_1^\xi(A), B_2 \in F_2^\xi(A)} \left\{ \frac{\langle B_1 - A, B_2 - A \rangle}{\|B_1 - A\|_F \|B_2 - A\|_F} \right\}, \quad (3)$$

with

$$F_1^\xi(A) = \{B_1 \mid B_1 \in \mathcal{M}_1 \setminus A, \|B_1 - A\|_F \leq \xi, B_1 - A \perp T_{\mathcal{M}_1 \cap \mathcal{M}_2}(A)\},$$

$$F_2^\xi(A) = \{B_2 \mid B_2 \in \mathcal{M}_2 \setminus A, \|B_2 - A\|_F \leq \xi, B_2 - A \perp T_{\mathcal{M}_1 \cap \mathcal{M}_2}(A)\},$$

and $T_{\mathcal{M}_1 \cap \mathcal{M}_2}(A)$ is the tangent space of $\mathcal{M}_1 \cap \mathcal{M}_2$ at point A . Based on this definition, a point $A \in \mathcal{M}_1 \cap \mathcal{M}_2$ is called a nontrivial intersection point when the angle is well defined. In addition, A is tangential if $\alpha(A) = 0$ and nontangential if $\alpha(A) > 0$. Andersson and Carlsson [2] showed that if A is a nontangential intersection point of \mathcal{M}_1 and \mathcal{M}_2 , there exist an $r > 0$, such that for any point $B \in \mathcal{B}(A, r)$, the sequence of alternating projections

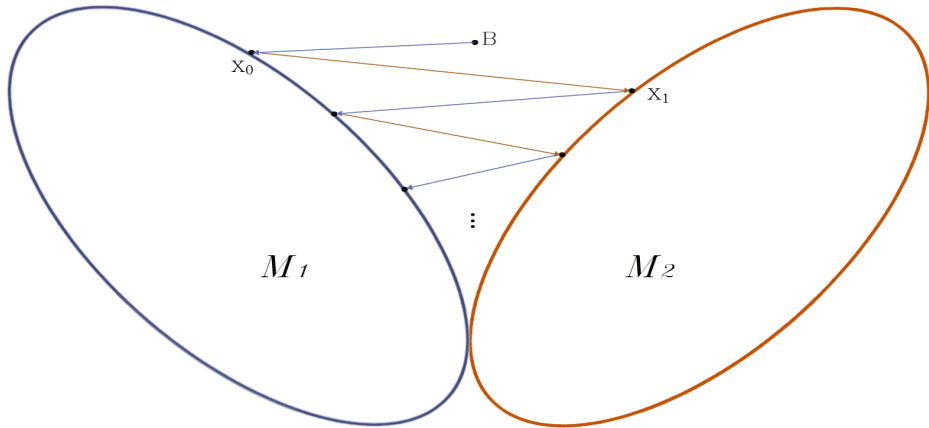
$$X_0 = \pi_1(B), X_1 = \pi_2(X_0), X_2 = \pi_1(X_1), X_3 = \pi_2(X_2), \dots,$$

convergent to a point on $\mathcal{M} = \mathcal{M}_1 \cap \mathcal{M}_2$, which is fairly close to the optimal point $\pi(B)$, see Figure 1(a). In addition, the convergence rate is proved to be decided by the angle between the two manifolds.

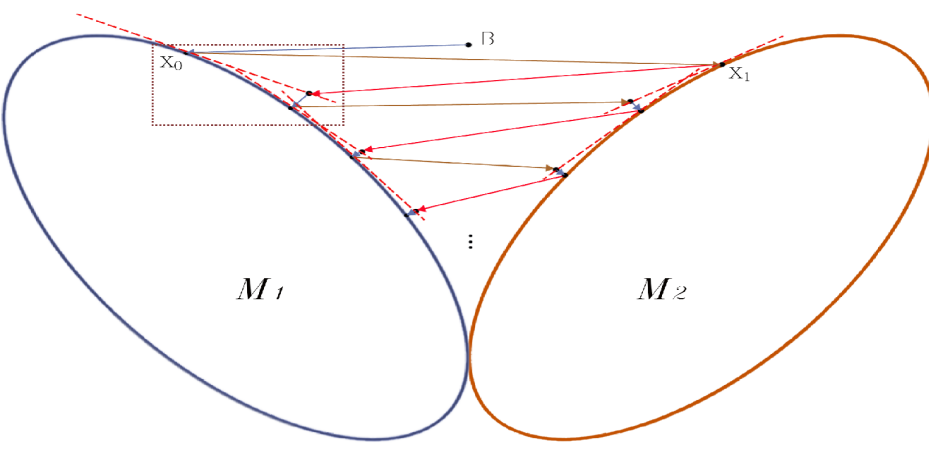
2.3 Projections Based on Tangent Spaces

Alternating Projection (AP) method updates the sequence by projecting an initial point back and forth between two manifolds. However, it can be computational expensive when a point is directly projected onto a manifold. For example, it is expensive to project a matrix onto the fixed rank manifold by the singular value decomposition (SVD) with a truncation out small singular values. Thus it is meaningful to find some new algorithm to reduce the computation complexity. Note that matrix manifold algorithms based on the tangent space have been widely studied in the literature (see for instance [5, 29] and their references therein). These works motivated us to propose a Tangent spaces-based Alternating Projection (TAP) method to reduce the computational cost.

In Figure 1 and Figure 2, we demonstrate the proposed TAP method. In the method, the given point B was first projected onto the manifold \mathcal{M}_1 to get a point X_0 by π_1 , and then X_1 is derived by projecting X_0 onto the manifold \mathcal{M}_2 by π_2 .



(a)



(b)

Figure 1: The comparison between (a) the AP method and (b) the proposed TAP method.

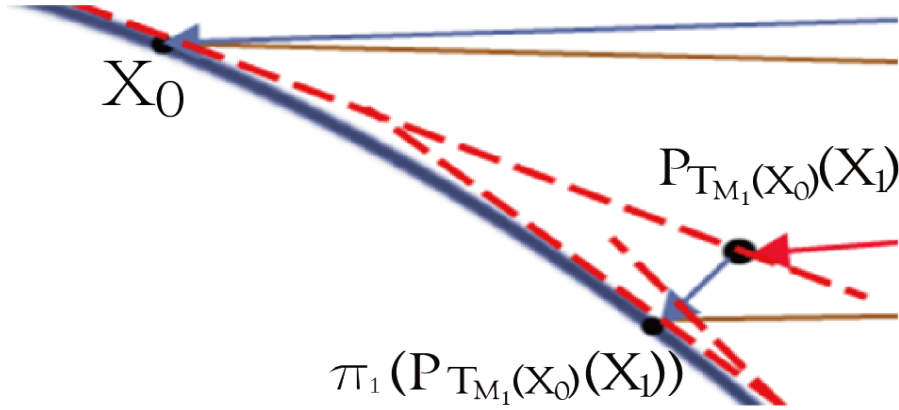


Figure 2: The zoomed region in Figure 1(b).

The first two steps are same as the usual AP method given in [21] and [2]. From the third step, the point X_1 is first projected onto the tangent space at X_0 of the manifold \mathcal{M}_1 by the orthogonal projection $P_{T_{\mathcal{M}}(X_0)}$, and then the derived point is projected from the tangent space to the manifold to get the point X_2 , after that the iterative sequence can be derived by similar projection method, which can be expressed as:

$$X_0 = \pi_1(B), X_1 = \pi_2(X_0), X_2 = \pi_1(P_{T_{\mathcal{M}_1}(X_0)}(X_1)), X_3 = \pi_2(P_{T_{\mathcal{M}_2}(X_1)}(X_2)), \dots, \quad (4)$$

where $P_{T_{\mathcal{M}}(X_{i-1})}(X_i)$, $i = 1, \dots$, denotes the orthogonal projections of X_i onto the tangent space of \mathcal{M} at points X_{i-1} , respectively. The proposed TAP method is given as the following algorithm.

Algorithm 1 Tangent spaces-based Alternating Projection (TAP) Method

Input: Given a point $A \in \mathcal{B}(A_0, s)$, this algorithm computes the point on $\mathcal{M}_1 \cap \mathcal{M}_2$ nearest $\pi(A)$.

- 1: Initialize $X_0 = A$;
- 2: $X_1 = \pi_1(X_0)$ and $Y_1 = \pi_2(X_1)$
- 3: for $k=1,2,\dots$,
- 4: $X_{k+1} = \pi_1(P_{T_{\mathcal{M}_1}(X_k)}(Y_k))$;
- 5: $Y_{k+1} = \pi_2(P_{T_{\mathcal{M}_2}(Y_k)}(X_{k+1}))$;
- 6: **end**

Output: X_k when the stopping criterion is satisfied.

2.4 Nonnegative Low Rank Matrix Approximation

In this subsection, we demonstrate the proposed method by considering nonnegative low rank matrix approximation. The nonnegative low rank matrix approximation is recently studied by Song and Ng in [27]. The aim is to find a nonnegative low rank matrix X such that $X \approx A$ such that their difference is as small as possible. Mathematically, it can be formulated as the following optimization problem

$$\min_{\text{rank}(X)=r, X \geq 0} \|A - X\|_F^2. \quad (5)$$

In [27], Song and Ng developed nonnegative low rank matrix approximation by using the alternating projections on the $m \times n$ fixed-rank matrices manifold

$$\mathcal{M}_r := \{X \in \mathbb{R}^{m \times n}, \text{rank}(X) = r\}, \quad (6)$$

and the $m \times n$ non-negativity matrices manifold

$$\mathcal{M}_n := \{X \in \mathbb{R}^{m \times n}, X_{i,j} \geq 0, i = 1, \dots, m, j = 1, \dots, n\}. \quad (7)$$

The projection onto the fixed rank matrix set \mathcal{M}_r is derived by the Eckart-Young-Mirsky theorem [10] which can be expressed as

$$\pi_1(X) = \sum_{i=1}^r \sigma_i(X) u_i(X) v_i^T(X), \quad (8)$$

where $\sigma_i(X)$ are first r singular values of X , and $u_i(X), v_i(X)$ are first r columns of the unitary matrices of $U(X)$ and $V(X)$. The projection onto the nonnegative matrix set \mathcal{M}_n is expressed as

$$\pi_2(X) = \begin{cases} X_{ij}, & \text{if } X_{ij} \geq 0, \\ 0, & \text{if } X_{ij} < 0. \end{cases} \quad (9)$$

Then the sequence derived by the alternating projection method is convergent to a point on the intersection of the two manifolds

$$\mathcal{M}_r \cap \mathcal{M}_n = \{X \in \mathbb{R}^{m \times n}, \text{rank}(X) = r, X_{ij} \geq 0, i = 1, \dots, m, j = 1, \dots, n\}, \quad (10)$$

which is sufficiently close to the best nonnegative approximation, see [27]. The main computational cost the above alternating projection method is to obtain the singular value decomposition $\pi_1(X)$ at each iteration.

Let us consider the proposed TAP for solving nonnegative low rank matrix approximation problem. Suppose that $k \geq 1$, X_k and Y_k are two consecutive terms in the sequence which are located on the manifold \mathcal{M}_r and \mathcal{M}_n respectively in Algorithm 1. Let $X_k = U_k \Sigma_k V_k^T$ be the skinny SVD decomposition of X_k . It follows the results in [1] that the tangent space of \mathcal{M}_r at X_k can be expressed as

$$T_{\mathcal{M}_r(X_k)} = \{U_k W^T + Z V_k^T \mid W, Z \in \mathbb{R}^{n \times r} \text{ are arbitrary}\}. \quad (11)$$

For the given iterate Y_k , it can be easily derived that the projections of Y_k onto the subspace $T_{\mathcal{M}_r(X_k)}$ and its orthogonal complement can be written as

$$P_{T_{\mathcal{M}_r(X_k)}}(Y_k) = U_k U_k^T Y_k + Y_k V_k V_k^T - U_k U_k^T Y_k V_k V_k^T,$$

and

$$(I - P_{T_{\mathcal{M}_r(X_k)}})(Y_k) = (I - U_k U_k^T) Y_k (I - V_k V_k^T).$$

Then $X_{k+1} = \pi_1(P_{T_{\mathcal{M}_r(X_k)}}(Y_k))$ can be derived by projecting $P_{T_{\mathcal{M}_r(X_k)}}(Y_k)$ from the tangent space $T_{\mathcal{M}_r(X_k)}$ to the manifold \mathcal{M}_r , where π_1 is defined as (8). Compared with the AP method given in [27], although an intermediate process is added in the TAP method, the matrix can be projected onto the \mathcal{M}_r from a low dimensional subspaces which can reduce computational cost. Computing the best rank- r approximation of a non-structured $n \times n$ matrix, costs $O(n^2 r) + n^2$ flops with a large hidden constant in front of $n^2 r$. In the proposed TAP method, the estimate of X_{k+1} can be computed in a very efficient way. Suppose that the QR decompositions of $(I - U_k U_k^T) Y_k V_k$ and $(I - V_k V_k^T) Y_k U_k$ are given as follows:

$$(I - U_k U_k^T) Y_k V_k = Q_k R_k \text{ and } (I - V_k V_k^T) Y_k U_k = \hat{Q}_k \hat{R}_k,$$

respectively. Recall that $U_k^T Q_k = V_k^T \hat{Q}_k = 0$ and then by a direct computation, we have

$$\begin{aligned} & P_{T_{\mathcal{M}_r(X_k)}}(Y_k) \\ &= U_k U_k^T Y_k (I - V_k V_k^T) + (I - U_k U_k^T) Y_k V_k V_k^T + U_k U_k^T Y_k V_k V_k^T \\ &= U_k \hat{R}_k^T \hat{Q}_k^T + Q_k R_k V_k^T + U_k U_k^T Y_k V_k V_k^T \\ &= \begin{pmatrix} U_k & Q_k \end{pmatrix} \begin{pmatrix} U_k^T Y_k V_k & \hat{R}_k^T \\ R_k & 0 \end{pmatrix} \begin{pmatrix} V_k^T \\ \hat{Q}_k^T \end{pmatrix} \\ &=: \begin{pmatrix} U_k & Q_k \end{pmatrix} M_k \begin{pmatrix} V_k^T \\ \hat{Q}_k^T \end{pmatrix}. \end{aligned}$$

Let $M_k = \Psi_k \Gamma_k \Phi_k^T$ be the SVD of M_k which can be computed using $O(r^3)$ flops since M_k is a $2r \times 2r$ matrix. Note that $\begin{pmatrix} U_k & Q_k \end{pmatrix}$ and $\begin{pmatrix} V_k & \hat{Q}_k \end{pmatrix}$ are orthogonal, then the SVD of $P_{T_{\mathcal{M}_r(X_k)}}(Y_k) = \Omega_k \Theta_k \Upsilon_k^T$ can be computed by

$$\Omega_k = \begin{pmatrix} U_k & Q_k \end{pmatrix} \Psi_k, \quad \Theta_k = \Gamma_k \text{ and } \Upsilon_k = \begin{pmatrix} V_k & \hat{Q}_k \end{pmatrix} \Phi_k.$$

It follows that the overall computational cost of $\pi_1(P_{T_{\mathcal{M}_r(X_k)}}(Y_k))$ can be expressed as two matrix-matrix multiplications between an $n \times n$ matrix and an $n \times r$ matrix, the QR decomposition of two $n \times r$ matrices, and SVD of a $2r \times 2r$ matrix, and a few matrix-matrix multiplications between a $r \times n$ matrix and an $n \times r$ matrix or between an $n \times r$ matrix and a $r \times r$ matrix, which leading to a total of $4n^2 r + O(r^2 n + r^3)$ flops. The computational cost of each iteration of TAP method is less than that of AP method.

3 The Convergence Analysis

In this section, we would like to show the convergence of the proposed TAP method. We begin this section with some results given in [2] which are necessary for the proof of the convergence of Algorithm 1. The following lemma says that the affine tangent-spaces are close to the manifold locally.

Lemma 3.1 (Proposition 2.4 in [2]). *Let \mathcal{M} be a \mathbb{C}^2 -manifold and $A \in \mathcal{M}$ be given. For each $\epsilon > 0$, there exists $s > 0$ such that for all $C \in \mathcal{B}(A, s) \cap \mathcal{M}$, we have:*

- (i) $\text{dist}(D, \tilde{T}_{\mathcal{M}}(C)) \leq \epsilon \|D - C\|_F, \forall D \in \mathcal{B}(A, s) \cap \mathcal{M}$.
- (ii) $\text{dist}(D, \mathcal{M}) \leq \epsilon \|D - C\|_F, \forall D \in \mathcal{B}(A, s) \cap \tilde{T}_{\mathcal{M}}(C)$.

Let $\rho_j(B) := P_{T_{\mathcal{M}_j}(\pi(B))}(B)$, $j = 1, 2$ denote the maps that project $B \in \mathcal{B}(A, s)$ onto the tangent spaces of the manifolds \mathcal{M}_1 and \mathcal{M}_2 at the intersection point $\pi(B)$, respectively. Then the following results can be derived by Propositions 2.1 and 2.2.

Lemma 3.2 (Lemma 4.2 in [2]). *The functions ρ_1 and ρ_2 are \mathbb{C}^1 -maps in $\mathcal{B}(A, s_0)$. Moreover, we can select a number $s_1^\epsilon < s_0^\epsilon$ such that the image of $\mathcal{B}(A, s_1^\epsilon)$ under $\rho_1, \rho_2, \pi, \pi_1, \pi_2$ as well as any composition of two of those maps, is contained in $\mathcal{B}(A, s_0^\epsilon)$.*

It follows from the definitions of ρ_j and $\pi_j, j = 1, 2$, that ρ_j resembles π_j , but is slightly different. Andersson and Carlsson [2] estimated the difference between ρ_j and $\pi_j, j = 1, 2$, respectively.

Lemma 3.3 (Proposition 4.3 in [2]). *Suppose that $\epsilon > 0$ with $\frac{1+\epsilon}{\sqrt{1-\epsilon^2}} < 2$. Given any $B \in \mathcal{B}(A, s^\epsilon)$, we have*

$$\|\pi_j(B) - \rho_j(B)\|_F < 4\sqrt{\epsilon} \|B - \pi(B)\|_F, \quad j = 1, 2.$$

Different from the results given in Lemma 3.3, we need to estimate the distances of $\pi_j(B)$ and $P_{T_{\mathcal{M}_j}(C_j)}(B)$, where C_j is a point on the manifold \mathcal{M}_j and not necessary the intersection point of \mathcal{M}_1 and \mathcal{M}_2 for $j = 1, 2$. We only list the results where the proof is similar to the proof of Lemma 3.3 given in [2].

Lemma 3.4. *For each $\epsilon > 0$ with $\frac{1+\epsilon}{\sqrt{1-\epsilon^2}} < 2$. Given any $B \in \mathcal{B}(A, s^\epsilon)$ and $C_j \in \mathcal{M}_j$, we have*

$$\|\pi_j(B) - P_{T_{\mathcal{M}_j}(C_j)}(B)\|_F < 4\sqrt{\epsilon} \|B - C_j\|_F, \quad j = 1, 2.$$

The following results are used as the main tool to prove the convergence of the Alternating Projection method given in [2].

Lemma 3.5 (Theorem 4.1 in [2]). *For each $\epsilon > 0$, there exist an $s > 0$ such that for all $B \in \mathcal{B}(A, s)$, we have*

$$\|\pi(\pi_j(B)) - \pi(B)\|_F < \epsilon \|B - \pi(B)\|_F, \quad j = 1, 2. \quad (12)$$

We remark that for a given ϵ that the number s given in Lemma 3.5 may be different between the manifolds \mathcal{M}_1 and \mathcal{M}_2 . Here we choose s such that (2) holds in all cases. Moreover, the roles of π_1 and π_2 , \mathcal{M}_1 and \mathcal{M}_2 in the proposed TAP method are equivalent, so we choose π_1 and \mathcal{M}_1 as a special case. Then we can get the following results.

Lemma 3.6. *For each $\epsilon > 0$ given in Lemma 3.4, there exist $\alpha(\epsilon) > 0$, $\beta(\epsilon) > 0$ and $s > 0$ such that for all $B \in \mathcal{B}(A, s)$,*

$$\|\pi(\pi_1(P_{T_{\mathcal{M}_1}(C)}(B))) - \pi(B)\|_F < \alpha(\epsilon)\|B - \pi(B)\|_F + \beta(\epsilon)\|C - \pi(B)\|_F, \quad (13)$$

where $C \in \mathcal{M}_1 \cap \mathcal{B}(A, s)$, π_1, π and $P_{T_{\mathcal{M}_1}(C)}$ stands for the projection onto \mathcal{M}_1 , \mathcal{M} and the tangent space $T_{\mathcal{M}_1}(C)$, respectively.

Proof. From Figure 1, we know that in the third step of the TAP method, the given point is projected onto the tangent space of $C \in \mathcal{M}_1$, i.e., $T_{\mathcal{M}_1}(C)$, instead of onto \mathcal{M}_1 directly. It follows Lemma 3.4 that for a given $\epsilon > 0$ with $\frac{1+\epsilon}{\sqrt{1-\epsilon^2}} < 2$, there exist an $s^\epsilon > 0$ such that for any $B \in \mathcal{B}(A, s^\epsilon)$, $\pi_1(P_{T_{\mathcal{M}_1}(C)}(B))$ resembles $\pi_1(B)$, i.e.,

$$\|\pi_1(B) - P_{T_{\mathcal{M}_1}(C)}(B)\|_F < 4\sqrt{\epsilon}\|B - C\|_F.$$

Recall Lemma 3.5 and note that $\pi_1(B) \in \mathcal{M}_1$, then for each ϵ^ϵ there exist an $s^\epsilon > 0$ such that for all $B \in \mathcal{B}(A, s^\epsilon)$, we have

$$\|\pi(\pi_1(B)) - \pi(B)\|_F < \epsilon^\epsilon\|B - \pi(B)\|_F.$$

$\pi_1(P_{T_{\mathcal{M}_1}(C)}(B))$ and $\pi_1(B)$ are all on the manifold \mathcal{M}_1 , and $\pi_1(P_{T_{\mathcal{M}_1}(C)}(B))$ is the closest point to $P_{T_{\mathcal{M}_1}(C)}(B)$ on the manifold \mathcal{M}_1 , then

$$\|P_{T_{\mathcal{M}_1}(C)}(B) - \pi_1(P_{T_{\mathcal{M}_1}(C)}(B))\|_F \leq \|P_{T_{\mathcal{M}_1}(C)}(B) - \pi_1(B)\|_F. \quad (14)$$

It follows from Lemma 3.2 that there exist an s^ϵ such that π is \mathbb{C}^2 in $\mathcal{B}(A, s^\epsilon)$. Choose $s = \min(s^\epsilon, s^\epsilon)$, then for all $B \in \mathcal{B}(A, s)$,

$$\begin{aligned} & \|\pi(\pi_1(P_{T_{\mathcal{M}_1}(C)}(B))) - \pi(B)\|_F \\ &= \|\pi(\pi_1(P_{T_{\mathcal{M}_1}(C)}(B))) - \pi(\pi_1(B)) + \pi(\pi_1(B)) - \pi(B)\|_F \\ &\leq \|\pi(\pi_1(P_{T_{\mathcal{M}_1}(C)}(B))) - \pi(\pi_1(B))\|_F + \|\pi(\pi_1(B)) - \pi(B)\|_F \\ &\leq \alpha\|\pi_1(P_{T_{\mathcal{M}_1}(C)}(B)) - \pi_1(B)\|_F + \epsilon\|B - \pi(B)\|_F \\ &\leq \alpha\|\pi_1(P_{T_{\mathcal{M}_1}(C)}(B)) - P_{T_{\mathcal{M}_1}(C)}(B) + P_{T_{\mathcal{M}_1}(C)}(B) - \pi_1(B)\|_F + \epsilon\|B - \pi(B)\|_F \\ &\leq \alpha\|\pi_1(P_{T_{\mathcal{M}_1}(C)}(B)) - P_{T_{\mathcal{M}_1}(C)}(B)\|_F + \alpha\|P_{T_{\mathcal{M}_1}(C)}(B) - \pi_1(B)\|_F + \epsilon\|B - \pi(B)\|_F \\ &\leq 2\alpha\|P_{T_{\mathcal{M}_1}(C)}(B) - \pi_1(B)\|_F + \epsilon\|B - \pi(B)\|_F \\ &\leq 8\alpha\sqrt{\epsilon}\|B - C\|_F + \epsilon\|B - \pi(B)\|_F \\ &\leq 8\alpha\sqrt{\epsilon}\|C - \pi(B)\|_F + (\epsilon + 8\alpha\sqrt{\epsilon})\|B - \pi(B)\|_F \\ &\leq \epsilon_1^1\|B - \pi(B)\|_F + \epsilon_2^1\|C - \pi(B)\|_F. \end{aligned}$$

The first part of the second inequality follows by the continuity of π , and the second part follows by Lemma 3.5. The first part of the fifth inequality as well as the sixth inequality follows by (14) and Lemma 3.4, respectively. Then the last inequality can be derived by choosing $\varepsilon + 8\alpha\sqrt{\varepsilon} \leq \varepsilon_1^\varepsilon$ and $8\alpha\sqrt{\varepsilon} \leq \varepsilon_2^\varepsilon$. In particular, if $B = \pi_2(C)$, we can get $\varepsilon_1^\varepsilon = \varepsilon$ and $\varepsilon_2^\varepsilon = 8\alpha\sqrt{\varepsilon}$. \square

Recall the function $\sigma(A)$ given in (3), the following results show that the distances between $\pi_j(B)$ ($j = 1, 2$) and $\pi(B)$ are reduced in proportion to the angle between \mathcal{M}_1 and \mathcal{M}_2 .

Lemma 3.7 (Theorem 4.5 in [2]). *For each $c > \sigma(A)$, there exist an $s > 0$ such that for all $B \in \mathcal{M}_2 \cap \mathcal{B}(A, s)$, we have*

$$\|\pi_1(B) - \pi(B)\|_F < c\|B - \pi(B)\|_F. \quad (15)$$

Moreover, the same holds true with the roles of \mathcal{M}_1 and \mathcal{M}_2 reversed.

In our case, the given point B is firstly projected onto the tangent space of \mathcal{M}_1 at C by the projector $P_{T_{\mathcal{M}_1}(C)}$, and then the derived point $P_{T_{\mathcal{M}_1}(C)}(B)$ is projected from the tangent space to the manifold to get $\pi_1(P_{T_{\mathcal{M}_1}(C)}(B))$. Then the distance between $\pi_1(P_{T_{\mathcal{M}_1}(C)}(B))$ and $\pi(B)$, can be estimated as follows.

Lemma 3.8. *Suppose that $C \in \mathcal{M}_1$ and $B = \pi_2(C) \in \mathcal{M}_2$, for each $c > \sigma(A)$, there exist an $s > 0$ such that for all $P_{T_{\mathcal{M}_1}(C)}(B) \in T_{\mathcal{M}_1}(C) \cap \mathcal{B}(A, s)$, we have*

$$\|\pi_1(P_{T_{\mathcal{M}_1}(C)}(B)) - \pi(B)\|_F < c\|B - \pi(B)\|_F. \quad (16)$$

Moreover, the same holds true with the roles of \mathcal{M}_1 and \mathcal{M}_2 reversed.

Proof. By Proposition 2.1 and Lemma 3.2, there exist an s_0 such that $P_{T_{\mathcal{M}_1}}, P_{T_{\mathcal{M}_1 \cap \mathcal{M}_2}}$ and π are continuous functions on $\mathcal{B}(A, s_0)$. Hence, we can pick $\alpha > 0$ such that

$$\|P_{T_{\mathcal{M}_1}}(B) - P_{T_{\mathcal{M}_1}}(B')\|_F \leq \alpha\|B - B'\|_F, \|\pi(B) - \pi(B')\|_F \leq \alpha\|B - B'\|_F$$

and

$$\|P_{T_{\mathcal{M}_1 \cap \mathcal{M}_2}}(B) - P_{T_{\mathcal{M}_1 \cap \mathcal{M}_2}}(B')\|_F \leq \alpha\|B - B'\|_F,$$

for all $B, B' \in \mathcal{B}(A, s_0)$. Fix c_1 such that $\sigma(A) < c_1 < c$, and pick an $s_1 < s_0$ such that

$$\sup\{\sigma(Z) : Z \in \mathcal{M}_1 \cap \mathcal{M}_2 \cap \mathcal{B}(A, s_1)\} < c_1$$

Let $c_2 > 1$ such that $c_2 c_1 < c$. Fix ε such that

$$\frac{1 + \varepsilon}{\sqrt{1 - \varepsilon^2}} < 2, \quad 8\sqrt{\varepsilon}(2 + \alpha) \frac{c_2}{c_2 - 1} \|C\|_F < c\|B\|_F \quad \text{and} \quad (1 + 4\sqrt{\varepsilon})c_2 c_1 < c. \quad (17)$$

Then fix $s < s_1$ such that

$$\pi(\mathcal{B}(A, s)) \subset \mathcal{B}(A, s_1),$$

and let $B \in \mathcal{B}(A, s) \cap \mathcal{M}_2$. There is no restriction to assume that $\pi(B) = 0$, which we do from now on. Note that $\pi(B) \in \mathcal{M}_1 \cap \mathcal{M}_2 \cap \mathcal{B}(A, s_1)$, so $\sigma(0) = \sigma(\pi(B)) < c_1$. In order to show

$$\frac{\|\pi_1(P_{T_{\mathcal{M}_1}(C)}(B)) - \pi(B)\|_F}{\|B - \pi(B)\|_F} = \frac{\|\pi_1(P_{T_{\mathcal{M}_1}(C)}(B))\|_F}{\|B\|_F} < c,$$

we need the following auxiliary information. Setting $B' = P_{T_{\mathcal{M}_2}(\pi(B))}(B)$, $D = \pi_1(B)$, $D' = P_{T_{\mathcal{M}_2}(\pi(B))}(B')$ and $E = \pi_1(P_{T_{\mathcal{M}_1}(C)}(B))$, then it is sufficient to show

$$\frac{\|\pi_1(P_{T_{\mathcal{M}_1}(C)}(B))\|_F}{\|B\|_F} = \frac{\|E\|_F}{\|D'\|_F} \frac{\|B'\|_F}{\|B\|_F} \frac{\|D'\|_F}{\|B'\|_F} < c.$$

The values of the three fractions $\frac{\|E\|_F}{\|D'\|_F}$, $\frac{\|B'\|_F}{\|B\|_F}$ and $\frac{\|D'\|_F}{\|B'\|_F}$ will be derived independently in the sequel. Recall the definition of B' and by Lemma 3.3, we have

$$\|B - B'\|_F = \|\pi_2(B) - B'\|_F < 4\sqrt{\epsilon}\|B - \pi(B)\|_F.$$

Similar to proof of Theorem 4.5 in [2], we can get

$$\frac{\|B'\|_F}{\|B\|_F} \leq 1 + 4\sqrt{\epsilon}, \quad \frac{\|D'\|_F}{\|B\|_F} \leq c_1 \quad (18)$$

and

$$\begin{aligned} \|D - D'\|_F &= \|\rho_1(B') - \pi_1(B)\|_F \leq \|\rho_1(B') - \rho_1(B)\|_F + \|\rho_1(B) - \pi_1(B)\|_F \\ &\leq \alpha\|B' - B\|_F + 4\sqrt{\epsilon}\|B\|_F = 4\sqrt{\epsilon}(1 + \alpha)\|B\|_F, \end{aligned}$$

respectively. For $\frac{\|E\|_F}{\|D'\|_F}$,

$$\begin{aligned} \|E - D'\|_F &= \|E - D + D - D'\|_F \leq \|E - D\|_F + \|D - D'\|_F \\ &= \|E - P_{T_{\mathcal{M}_1}(C)}(B) + P_{T_{\mathcal{M}_1}(C)}(B) - D\|_F + \|D - D'\|_F \\ &\leq \|E - P_{T_{\mathcal{M}_1}(C)}(B)\|_F + \|P_{T_{\mathcal{M}_1}(C)}(B) - D\|_F + \|D - D'\|_F \\ &= \|\pi_1(P_{T_{\mathcal{M}_1}(C)}(B)) - P_{T_{\mathcal{M}_1}(C)}(B)\|_F + \|P_{T_{\mathcal{M}_1}(C)}(B) - \pi_1(B)\|_F \\ &\quad + \|\pi_1(B) - D'\|_F. \end{aligned} \quad (19)$$

By Lemma 3.4, and note that $B = \pi_2(C)$, $\pi(B)$ are all on \mathcal{M}_2 , then

$$\|P_{T_{\mathcal{M}_1}(C)}(B) - \pi_1(B)\|_F < 4\sqrt{\epsilon}\|B - C\|_F \leq 4\sqrt{\epsilon}\|C - \pi(B)\|_F. \quad (20)$$

Similarly, $\pi_1(P_{T_{\mathcal{M}_1}(C_1)}(B))$ and $\pi_1(B)$ are all on \mathcal{M}_1 , thus

$$\|\pi_1(P_{T_{\mathcal{M}_1}(C)}(B)) - P_{T_{\mathcal{M}_1}(C)}(B)\|_F \leq \|P_{T_{\mathcal{M}_1}(C)}(B) - \pi_1(B)\|_F \leq 4\sqrt{\epsilon}\|C - \pi(B)\|_F. \quad (21)$$

Combining (19), (20) and (21), we have

$$\begin{aligned} \|E - D'\|_F &< 4\sqrt{\epsilon}\|C - \pi(B)\|_F + 4\sqrt{\epsilon}\|C - \pi(B)\|_F + 4\sqrt{\epsilon}(1 + \alpha)\|B - \pi(B)\|_F \\ &= 8\sqrt{\epsilon}\|C - \pi(B)\|_F + 4\sqrt{\epsilon}(1 + \alpha)\|B - C + C - \pi(B)\|_F \\ &\leq 8\sqrt{\epsilon}\|C - \pi(B)\|_F + 4\sqrt{\epsilon}(1 + \alpha)(\|B - C\|_F + \|C - \pi(B)\|_F)v \\ &< 8\sqrt{\epsilon}\|C - \pi(B)\|_F + 8\sqrt{\epsilon}(1 + \alpha)\|C - \pi(B)\|_F \\ &= (2 + \alpha)8\sqrt{\epsilon}\|C - \pi(B)\|_F. \end{aligned} \quad (22)$$

For the value of $\frac{\|E\|_F}{\|D'\|_F}$, there exist two case: one case is $\frac{\|E\|_F}{\|D'\|_F} \leq c_2$ and the other one is $\frac{\|E\|_F}{\|D'\|_F} > c_2$. If the later case is satisfied, by (22), we have

$$\begin{aligned} \|E\|_F - \|D'\|_F &< \|E - D'\|_F < (2 + \alpha)8\sqrt{\epsilon}\|C\|_F \\ \Rightarrow (c_2 - 1)\|D'\|_F &< (2 + \alpha)8\sqrt{\epsilon}\|C\|_F \Rightarrow \|E\|_F < \frac{c_2}{c_2 - 1}(2 + \alpha)8\sqrt{\epsilon}\|C\|_F. \end{aligned} \quad (23)$$

Then a suitable ϵ can be chosen such that

$$\frac{c_2}{c_2 - 1}(2 + \alpha)8\sqrt{\epsilon}\|C\|_F < c\|B\|_F,$$

in which case we are done. For the other case, combining the results in (18) and $\frac{\|E\|_F}{\|D'\|_F} \leq c_2$, we can get

$$\frac{\|E\|_F}{\|B\|_F} = \frac{\|E\|_F}{\|D'\|_F} \frac{\|B'\|_F}{\|B\|_F} \frac{\|D'\|_F}{\|B'\|_F} < (1 + 4\sqrt{\epsilon})c_2c_1 < c,$$

where the second inequality follows by (17). \square

We can now list the main results as the following theorem.

Theorem 3.9. *Suppose that \mathcal{M}_1 , \mathcal{M}_2 and $\mathcal{M} = \mathcal{M}_1 \cap \mathcal{M}_2$ are \mathbb{C}^2 -manifold. Let A_0 be a nontangential point of $\mathcal{M}_1 \cap \mathcal{M}_2$. Then for any given ϵ and $1 > c > \sigma(A_0)$, there exist an $\xi > 0$ such that for any $A \in \mathcal{B}(A_0, \xi)$ (the ball neighborhood of A_0 with radius ξ) the sequence $\{X_k\}_{k=0}^\infty$ generated by the alternating projection algorithm initializing from given A :*

$$\begin{aligned} X_0 &= \pi_1(A), X_1 = \pi_2(X_0), X_2 = \pi_1(P_{T_{\mathcal{M}_1}(X_0)}(X_1)), X_3 = \pi_2(P_{T_{\mathcal{M}_2}(X_1)}(X_2)), \dots, \\ X_{2k} &= \pi_1(P_{T_{\mathcal{M}_1}(X_{2k-2})}(X_{2k-1})), X_{2k+1} = \pi_2(P_{T_{\mathcal{M}_2}(X_{2k-1})}(X_{2k})), \dots \end{aligned}$$

satisfies the following results:

(i) converges to a point $X_\infty \in \mathcal{M}_1 \cap \mathcal{M}_2$,

(ii) $\|X_\infty - \pi(A)\|_F \leq \epsilon \|A - \pi(A)\|_F$,

(iii) $\|X_\infty - X_k\|_F \leq \text{const} \cdot c^k \|A - \pi(A)\|_F$.

Proof. Assume that $\epsilon < 1$ and $\sigma(A_0) < c < 1$. Recall Lemma 3.6, set

$$\varepsilon_1 = \varepsilon = \frac{1-c}{2(3-c)}\epsilon, \quad \varepsilon_2 = \frac{1-c}{2+2\alpha}\epsilon,$$

where α is a constant given as in the proof of Lemma 3.8. Moreover, there exist some possibly distinct radii that guarantee Lemma 3.7-3.8 are satisfied. Let s denote the minimum of these possibly radii and pick $r < \frac{s(1-\epsilon)}{4(2+\epsilon)}$, so that $\pi(\mathcal{B}(A_0, r)) \subseteq \mathcal{B}(A_0, s/4)$. Then $\|\pi(A) - A_0\|_F < s/4$ follows from the latter condition. Denote $l = \|A - \pi(A)\|_F$, and note that

$$l = \|A - A_0 + A_0 - \pi(A)\|_F \leq \|A - A_0\|_F + \|A_0 - \pi(A)\|_F \leq r + s/4.$$

As $\pi(A) \in \mathcal{M}_1 \cap \mathcal{M}_2$ and note that $X_0 = \pi_1(A)$, we have

$$\|X_0 - A\|_F = \|\pi_1(A) - A\|_F \leq \|\pi(A) - A\|_F = l$$

and

$$\|X_0 - \pi(X_0)\|_F \leq \|X_0 - \pi(A)\|_F \leq \|X_0 - A\|_F + \|A - \pi(A)\|_F \leq 2l.$$

If

$$\{X_k\}_{k=0}^{k-1} \subseteq \mathcal{B}(A_0, s) \tag{24}$$

is satisfied, then by Lemma 3.8, we can get

$$\|X_k - \pi(X_k)\|_F \leq \|X_k - \pi(X_{k-1})\|_F \leq c \|X_{k-1} - \pi(X_{k-1})\|_F. \tag{25}$$

Next we will show (24) is satisfied by induction. Firstly, for $k = 0$,

$$\|X_0 - A_0\|_F \leq \|X_0 - A\|_F + \|A - A_0\|_F \leq l + r/2 \leq 2r + s/4 \leq \frac{s(1-\epsilon)}{2(2+\epsilon)} + s/4 < s.$$

Assume that (24) is satisfied when $n = k$, then it follows from (25) that

$$\|X_k - \pi(X_k)\|_F \leq c^k \|X_0 - \pi(X_0)\|_F \leq 2lc^k. \tag{26}$$

Note that

$$\begin{aligned} \|X_{k-2} - \pi(X_{k-1})\|_F &= \|X_{k-2} - \pi(\pi_2(X_{k-2}))\|_F \\ &= \|X_{k-2} - \pi(X_{k-2}) + \pi(X_{k-2}) - \pi(\pi_2(X_{k-2}))\|_F \\ &\leq \|X_{k-2} - \pi(X_{k-2})\|_F + \|\pi(X_{k-2}) - \pi(\pi_2(X_{k-2}))\|_F \\ &\leq \|X_{k-2} - \pi(X_{k-2})\|_F + \alpha \|X_{k-2} - \pi_2(X_{k-2})\|_F \\ &\leq (1 + \alpha) \|X_{k-2} - \pi(X_{k-2})\|_F. \end{aligned}$$

The second part of the second inequality follows by the continuous of the projection π , the third inequality follows by $\|X_{k-2} - \pi_2(X_{k-2})\|_F \leq \|X_{k-2} - \pi(X_{k-2})\|_F$. Applying Lemma 3.6 gives

$$\begin{aligned} \|\pi(X_k) - \pi(X_{k-1})\|_F &< \varepsilon_1 \|X_{k-1} - \pi(X_{k-1})\|_F + \varepsilon_2 \|X_{k-2} - \pi(X_{k-1})\|_F \\ &< \varepsilon_1 \|X_{k-1} - \pi(X_{k-1})\|_F + \varepsilon_2(1 + \alpha) \|X_{k-2} - \pi(X_{k-2})\|_F \\ &\leq 2\varepsilon_1 c^{k-1} l + 2\varepsilon_2(1 + \alpha) c^{k-2} l = (\varepsilon_1 c + \varepsilon_2(1 + \alpha)) 2c^{k-2} l. \end{aligned} \quad (27)$$

Recall Lemma 12 and the inequality derived in (27), we have

$$\begin{aligned} \|\pi(X_k) - \pi(A)\|_F &\leq \|\pi(A) - \pi(X_0)\|_F + \|\pi(X_1) - \pi(X_0)\|_F + \sum_{j=2}^k \|\pi(X_j) - \pi(X_{j-1})\|_F \\ &\leq \varepsilon l + 2\varepsilon l + \sum_{j=2}^k (\varepsilon_1 c + \varepsilon_2(1 + \alpha)) 2c^{j-2} l \\ &\leq 3\varepsilon l + \frac{2(\varepsilon_1 c + \varepsilon_2(1 + \alpha))}{1 - c} l = \frac{3\varepsilon(1 - c) + 2\varepsilon c + (1 + \alpha)\varepsilon_2}{1 - c} l \\ &\leq \varepsilon l. \end{aligned} \quad (28)$$

Thus,

$$\begin{aligned} \|A_0 - X_k\|_F &\leq \|A_0 - \pi(A)\|_F + \|\pi(A) - \pi(X_k)\|_F + \|\pi(X_k) - X_k\|_F \\ &\leq s/4 + \varepsilon l + 2l < s, \end{aligned}$$

which shows that (24) is satisfied.

It follows from (27) that the sequence $(\pi(B_k))_{k=1}^{\infty}$ is a Cauchy sequence, and then it converges to some point B_{∞} . Moreover, by (26) the sequence $(B_k)_{k=1}^{\infty}$ must also converge, and the limit point is also B_{∞} . It follows that $B_{\infty} = \pi(B_{\infty})$, then (i) is concluded. Moreover, by taking the limit (28) we can get (ii). For (iii). Note that

$$\|\pi(B_k) - B_{\infty}\|_F \leq \sum_{j=k+1}^{\infty} \|\pi(X_j) - \pi(X_{j-1})\|_F \leq \frac{2l\varepsilon c^k}{1 - c} + \frac{2(1 + \alpha)l\varepsilon_2 c^{k-1}}{1 - c}, \quad (29)$$

and combine with (26), we can get

$$\begin{aligned} \|B_k - B_{\infty}\|_F &\leq \|B_k - \pi(B_k)\|_F + \|\pi(B_k) - B_{\infty}\|_F \leq (2l + \frac{2l\varepsilon}{1 - c} + \frac{2(1 + \alpha)l\varepsilon_2}{1 - c}) c^k \\ &= \beta c^k l, \end{aligned}$$

with a constant β as desired. \square

In the next section, we will test the performance of the proposed TAP method.

4 Numerical Examples

In this section, numerical results are presented to show the effectiveness of the proposed TAP method (Algorithm 1). There are two kinds of examples to be tested: nonnegative low rank matrix approximation and low rank quaternion (color image) matrix approximation. All the experiments are performed under Windows 7 and MATLAB R2018a running on a desktop (Intel Core i7, @ 3.40GHz, 8.00G RAM).

4.1 Nonnegative Low Rank Matrix Approximation

In the first experiment, we randomly generated n -by- n nonnegative matrices A where their matrix entries follow a uniform distribution in between 0 and 1. We employed the proposed TAP method and AP method [27] to test the relative residual $\|A - X_c\|_F / \|A\|_F$, where X_c are the computed rank r solutions by different methods. For comparison, we also list the results by nonnegative matrix factorization algorithms: A-MU [9], A-HALS [9] and A-PG [18].

Tables 1 shows the relative residuals of the computed solutions from the proposed TAP method and the other testing methods for synthetic data sets of sizes 200-by-200, 400-by-400 and 800-by-800. Note that there is no guarantee that other testing NMF algorithms can determine the underlying nonnegative low rank factorization. In the tables, it is clear that the testing NMF algorithms cannot obtain the underlying low rank factorization. One of the reason may be that NMF algorithms can be sensitive to initial guesses. In the tables, we illustrate this phenomena by displaying the mean relative residual and the range containing both the minimum and the maximum relative residuals by using ten initial guesses randomly generated. We find in the table that the relative residuals computed by the TAP method is the same as those by the AP method. It implies that the proposed TAP method can achieve the same accuracy of classical alternating projection. According to the tables, the relative residuals by both TAP and AP methods are always smaller than the minimum relative residuals by the testing NMF algorithms. In addition, we report the computational time (seconds calculated by MATLAB) in the tables. We see that the computational time required by the proposed TAP method is less than that required by AP method.

Moreover, we considered the CBCL face database [32]. In the face database, there are $m = 2469$ facial images, each consisting of $n = 19 \times 19 = 361$ pixels, and constituting a face image matrix $A \in \mathbb{R}_+^{361 \times 2469}$. We tested several values of $r = 20, 40, 60, 80, 100$ for nonnegative low rank minimization and compared the proposed TAP method with the other algorithms. In the testing NMF algorithms, we used 10 different initial guesses and report the results of mean relative residuals in the table. We see from Table 2 that the relative residuals computed by the proposed TAP method and the AP method is smaller than the mean relative residuals by the testing NMF algorithms. Again the computational time required by the proposed TAP method is smaller than that by the AP method.

Table 1: The comparison of different algorithms.

Method	200-by-200 matrix		
	$r = 10$	$r = 20$	$r = 40$
TAP	0.4576	0.4161	0.3247
Time	0.42	0.48	0.38
AP	0.4576	0.4161	0.3247
Time	0.66	0.66	0.42
A-MU (mean)	0.4592	0.4249	0.3733
A-MU (range)	[0.4591, 0.4593]	[0.4246, 0.4251]	[0.3729, 0.3737]
Time (mean)	8.32	9.54	15.34
Time (range)	[8.00, 8.81]	[9.41, 9.61]	[14.72, 15.75]
A-HALS (mean)	0.4591	0.4246	0.3717
A-HALS (range)	[0.4590, 0.4593]	[0.4244, 0.4247]	[0.3714, 0.3719]
Time (mean)	1.09	1.95	4.01
Time (range)	[0.98, 1.22]	[1.86, 2.05]	[3.86, 4.13]
A-PG (mean)	0.4591	0.4244	0.3717
A-PG (range)	[0.4590,0.4592]	[0.4243, 0.4246]	[0.3715, 0.3719]
Time (mean)	14.77	16.24	21.52
Time (range)	[14.50,15.03]	[15.81, 16.55]	[21.02, 21.77]
Method	400-by-400 matrix		
	$r = 20$	$r = 40$	$r = 80$
TAP	0.4573	0.4161	0.3421
Time	1.55	1.32	1.10
AP	0.4573	0.4161	0.3421
Time	2.95	2.47	1.68
A-MU (mean)	0.4606	0.4301	0.3857
A-MU (range)	[0.4605, 0.4607]	[0.4300, 0.4302]	[0.3856, 0.3860]
Time (mean)	37.80	38.72	46.41
Time (range)	[36.67, 39.03]	[38.21, 39.18]	[45.87, 48.28]
A-HALS (mean)	0.4604	0.4295	0.3836
A-HALS (range)	[0.4603, 0.4605]	[0.4294, 0.4296]	[0.3833, 0.3838]
Time (mean)	3.10	7.40	19.67
Time (range)	[3.03, 3.25]	[7.12, 7.60]	[19.04, 20.61]
A-PG (mean)	0.4604	0.4297	0.3850
A-PG (range)	[0.4604, 0.4605]	[0.4296, 0.4298]	[0.3847, 0.3853]
Time (mean)	51.68	60.80	61.95
Time (range)	[51.04, 52.26]	[60.62, 61.01]	[61.34, 62.64]
Method	800-by-800 matrix		
	$r = 40$	$r = 80$	$r = 160$
TAP	0.4550	0.4144	0.3412
Time	7.14	4.84	4.80
AP	0.4550	0.4144	0.3412
Time	15.84	9.55	7.11
A-MU (mean)	0.4608	0.4350	0.3984
A-MU (range)	[0.4607, 0.4609]	[0.4349, 0.4351]	[0.3982, 0.3986]
Time (mean)	60.29	60.96	61.31
Time (range)	[60.03, 60.65]	[60.61, 61.58]	[60.72, 61.94]
A-HALS (mean)	0.4605	0.4336	0.3984
A-HALS (range)	[0.4604,0.4605]	[0.4335, 0.4336]	[0.3982, 0.3986]
Time (mean)	18.54	47.70	61.30
Time (range)	[17.76, 19.48]	[43.33, 52.75]	[60.71, 61.91]
A-PG (mean)	0.4606	0.4343	0.4007
A-PG (range)	[0.4606, 0.4607]	[0.4342, 0.4344]	[0.4005, 0.4012]
Time (mean)	60.38	61.26	61.76
Time (range)	[60.12, 60.79]	[60.78, 61.81]	[61.29 62.48]

Table 2: The relative residuals and computational time (in seconds) by different algorithms for face data matrix.

Method	361-by-2649 matrix				
	$r = 20$	$r = 40$	$r = 60$	$r = 80$	$r = 100$
TAP	0.1170	0.0839	0.0645	0.0529	0.0438
Time	26.27	13.97	9.98	7.87	7.26
AP	0.1170	0.0839	0.0645	0.0529	0.0438
Time	70.50	34.02	21.77	15.22	11.98
A-MU (mean)	0.1223	0.0923	0.0756	0.0645	0.0561
A-MU (range)	[0.1219, 0.1229]	[0.0918, 0.0934]	[0.0752, 0.0760]	[0.0640, 0.0649]	[0.0557, 0.0564]
Time (mean)	60.29	60.71	61.11	61.48	61.87
Time (range)	[60.03, 60.65]	[60.31, 60.17]	[60.81, 61.17]	[60.93, 62.01]	[61.42, 62.64]
A-HALS (mean)	0.1220	0.0919	0.0720	0.0595	0.0503
A-HALS (range)	[0.1218, 0.1223]	[0.0916, 0.0922]	[0.0718, 0.0722]	[0.0594, 0.0598]	[0.0502, 0.0505]
Time (mean)	21.62	39.40	54.88	61.22	105.97
Time (range)	[20.71, 22.78]	[38.34, 40.40]	[52.15, 59.98]	[60.73, 61.64]	[103.03, 107.45]
A-PG (mean)	0.1223	0.0901	0.0781	0.0687	0.0625
A-PG (range)	[0.1219, 0.1229]	[0.0899, 0.0904]	[0.0776, 0.0787]	[0.0682, 0.0692]	[0.0618, 0.0632]
Time (mean)	60.38	60.65	60.08	61.22	61.04
Time (range)	[60.09, 60.71]	[60.31, 61.17]	[60.51, 61.39]	[60.73, 61.64]	[60.71, 61.43]

4.2 Low Rank Color Image Approximation

Nowadays, color images appear commonly in many image processing applications. The use of quaternion matrices for color images representation has been studied in the literature, see [4, ?, 8, 15, 24, 25, 28]. A color image contains red, blue and green channels, the quaternion approach is to encode the red, green and blue channel pixel values on the three imaginary parts of a quaternion. The main advantage is that color images can be studied and processed holistically as a vector field, see [8, 25, 28]. We can make use of quaternion matrix to represent color images and study the optimal rank- r approximation of color image in terms of Frobenius norm. A low rank approximation of a purely quaternion matrix (red, green and blue channels color image) can be obtained by using the quaternion singular value decomposition [31]. However, this approximation may not be optimal in the sense that the resulting approximation matrix may not be purely quaternion, i.e., it may contain the real component and it is not referred to a color image. Here the following optimization problem is considered:

$$\min_{\text{rank}(\mathbf{X})=r, \text{Re}(\mathbf{X})=0} \|\mathbf{A} - \mathbf{X}\|_F^2, \quad (30)$$

where \mathbf{A} is a given purely quaternion matrix and $\text{Re}(\mathbf{X})$ stands for the real part of \mathbf{X} . Here, we employ two color images “peppafamily” and “pepper” with sizes 256×256 to compare TAP and AP in terms of residuals and time. The original color images and their ranks 6, 12, 18 and 24 approximations by TAP and AP methods are listed in Figure 3. We see from the figure that the low rank approximation of color images

Table 3: The relative residuals and computational time (in second) by different algorithms for two color image matrices.

Method	‘peppafamily’ color image matrix				‘pepper’ color image matrix			
	$r = 6$	$r = 12$	$r = 18$	$r = 24$	$r = 6$	$r = 12$	$r = 18$	$r = 24$
TAP	0.1321	0.1039	0.0861	0.0734	0.2267	0.1648	0.1317	0.1112
Time	240.25	448.58	710.58	930.01	270.44	458.05	754.25	919.98
AP	0.1320	0.1038	0.0861	0.0733	0.2267	0.1646	0.1317	0.1112
Time	6856.07	6709.38	7044.16	6609.02	6943.01	6654.63	6869.88	6545.88

by the TAP method and the AP method are about the same in terms of visual quality. Their relative residuals and their computation time are shown in the Table 3. According to the table, the relative residuals by both TAP and AP methods are nearly the same, however the computational time of the proposed TAP method is much less than that required by AP method.

5 Conclusion

In this paper, we study alternating projections on nontangential manifolds based on the tangent spaces. We have shown that the sequence generated by alternating projections on two nontangential manifolds based on tangent spaces, converges linearly to a point in the intersection of the two manifolds where the convergent point is close to the optimal solution. Numerical examples based nonnegative low rank matrix approximation and low rank image quaternion matrix (color image) approximation are given to demonstrate that the performance of the proposed method is better than that of the classical alternating projection method in terms of computational time.

As a future research work, it is interesting to study applications involved the projections of manifolds (for example face recognition). Moreover, In many applications, researchers have suggested to use the other norms (such as l_1 norm) in data fitting instead of Frobenius norm to deal with other machine learning applications. It is necessary to develop the related algorithms for such manifold optimization problems.

References

- [1] P. Absil, R. Mahony and R. Sepulchre, Optimization algorithms on matrix manifolds, Princeton University Press, 2009.
- [2] F. Andersson and M. Carlsson, *Alternating projections on nontangential manifolds*, *Constructive approximation*, 38 (2013) 489-525.
- [3] M. Berger and B. Gostiaux, *Differential Geometry: Manifolds, Curves and Surfaces*. Springer, Berlin, 2012.

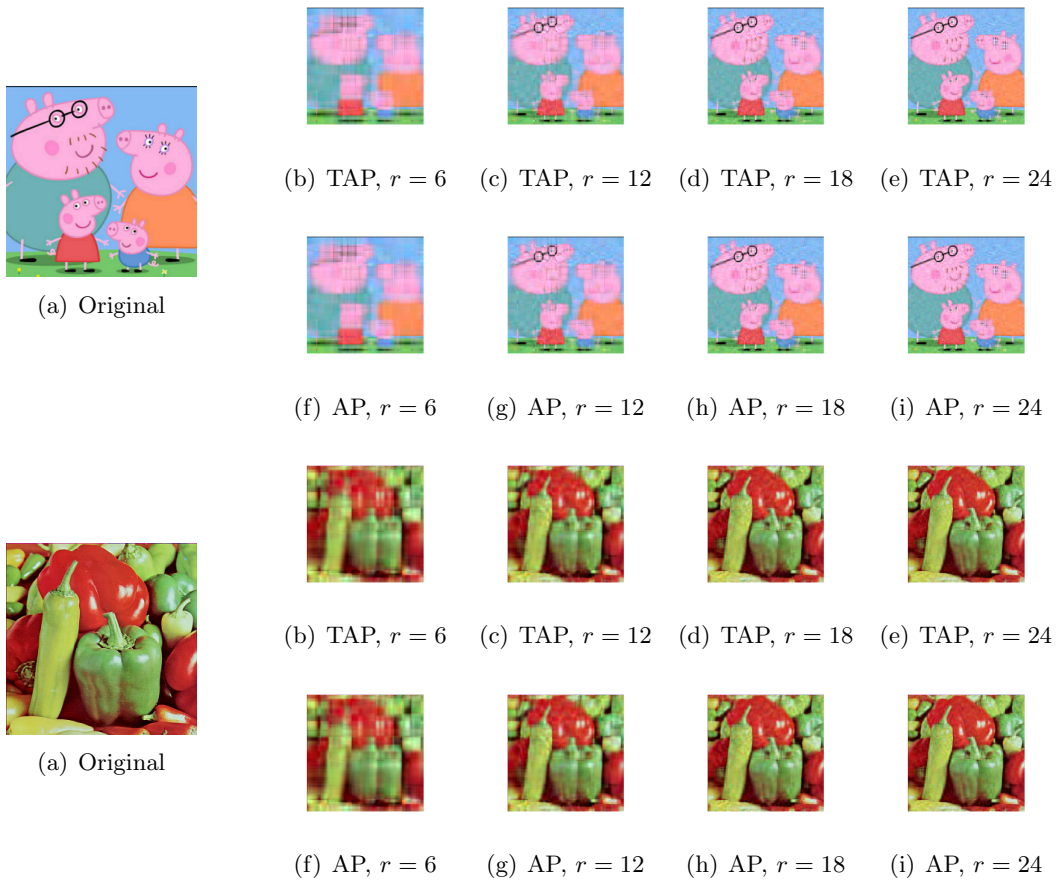


Figure 3: The rank 6, 12, 18, 24 approximations of ‘peppafamily’ and ‘pepper’ by TAP and AP methods, respectively

- [4] N. Bihan and J. Mars, *Singular value decomposition of quaternion matrices: a new tool for vector-sensor signal processing*, Signal processing, 84 (2004) 1177-1199.
- [5] H. Cai, J. Cai and K. Wei, *Accelerated alternating projections for robust principal component analysis*, Journal of machine learning research 20 (2019) 1-33.
- [6] X. Chen and M. Chu, *On the least squares solution of inverse eigenvalue problems*, SIAM J. Number. Anal. 33 (1996) 2417-2430.
- [7] P. Combettes, *Signal recovery by best feasible approximation*, IEEE transactions on Image Processing, 2 (1993) 269-271.
- [8] T. Ell and S. Sangwine, *Hypercomplex fourier transforms of color images*, IEEE Transactions on image processing, 16 (2006) 22–35.

- [9] N. Gillis and F. Glineur, *Accelerated multiplicative updates and hierarchical ALS algorithms for nonnegative matrix factorization*, *Neural computation* 24(4) (2012) 1085-1108.
- [10] G. Golub and C. Van Loan, *Matrix Computations*, vol. 3, JHU press, 2012.
- [11] K. Grigoriadis, A. Frazho and R. Skelton, *Application of alternating convex projection methods for computation of positive toeplitz matrices*, *IEEE transactions on signal processing*, 42 (1994) 1873-1875.
- [12] K. Grigoriadis and R. Skelton, *Low-order control design for LMI problems using alternating projection methods*, *Automatica* 32 (1996) 1117-1125.
- [13] K. Grigoriadis and E. Beran, *Alternating projection algorithms for linear matrix inequalities problem with rank constraints*, *Adv. Linear Matrix Inequality Methos in Control*, SIAM, Philadelphia, 256-267.
- [14] C. Hamaker and D. Solmon, *The angles between the null spaces of x rays*, *Journal of mathematical analysis and applications*, 62 (1978) 1-23.
- [15] X. Han, J. Wu, L. Yan, L. Senhadji and H. Shu, *Color image recovery via quaternion matrix completion*, in 2013 6th International Congress on Image and Signal Processing (CISP), vol. 1, IEEE (2013), 358–362.
- [16] N. Higham, *Computing the nearest correlation matrix – a problem from finance*, *IMA journal of Numerical Analysis*, 22 (2002) 329–343.
- [17] S. Kayalar and H. Weinert, *Error bounds for the method of alternating projections*, *Mathematics of Control, Signals and Systems*, 1 (1988) 43–59.
- [18] C. Lin, *Projected gradient methods for nonnegative matrix factorization*, *Neural computation* 19(10) (2007) 2756-2779.
- [19] S. Lee, P. Cho, R. Marks and S. Oh, *Conformal radiotherapy computation by the method of alternating projections onto convex sets*, *Physics in Medicine & Biology*, 42 (1997) 1065.
- [20] A. Levi and H. Stark, *Signal restoration from phase by projections onto convex sets*, *JOSA*, 73 (1983) 810-822.
- [21] A. Lewis and J. Malick, *Alternating projections on manifolds*, *Mathematics of Operations Research*, 33 (2008) 216-234.
- [22] J. von Neumann, *Functional Operators*, vol. II: The Geometry of Orthogonal Spaces, Princeton University Press, Princeton, 1950.
- [23] R. Orsi, U. Helmke and J. Moore, *A Newton-like method for solving rank constrained linear matrix inequalityies*, *Automatica* 42 (2006) 1875-1882.

- [24] S. Pei, J. Ding and J. Chang, *Efficient implementation of quaternion fourier transform, convolution, and correlation by 2-d complex fft*, IEEE Transactions on Signal Processing, 49 (2001) 2783-2797.
- [25] S. Sangwine, *Fourier transforms of colour images using quaternion or hyper-complex numbers*, Electronics letters, 32 (1996) 1979-1980.
- [26] H. Schwarz, *Über einige Abbildungsaufgaben*, Gesammelte Mathematische Abhandlungen 11 (1869) 65-83.
- [27] G. Song and M. Ng, *Nonnegative Low Rank Matrix Approximation for Nonnegative Matrices*, Applied Mathematics Letter.
- [28] Ö. Subakan and B. Vemuri, *A quaternion framework for color image smoothing and segmentation*, International Journal of Computer Vision, 91 (2011) 233-250.
- [29] K. Wei, J. Cai, T. Chan and S. Leung, *Guarantees of Riemannian optimization for low rank matrix completion*, Inverse Problems and Imaging, 14(2) (2020) 233-265.
- [30] B. Widrow, *Adaptive inverse control*, in Adaptive Systems in Control and Signal Processing 1986, Elsevier, (1987) 1-5.
- [31] F. Zhang, *Quaternions and matrices of quaternions*, Linear algebra and its applications, 251 (1997) 21-57.
- [32] CBCL Face Database, *MIT Center For Biological and Computation Learning*, <http://www.ai.mit.edu/projects/cbcl>.